Journal of Applied Polymer Science

Synergistic Effect of Aluminum Hydroxide and Expandable Graphite on the Flame Retardancy of Polyisocyanurate–Polyurethane Foams

Wanjin Wang,[1,2] Kui He,[2] Quanxiao Dong,[2] Ning Zhu,[2] Yong Fan,[2] Feng Wang,[3] Yibing Xia,[2] Haifeng Li,[2] Jing Wang,[2] Zhen Yuan,[2] Erpo Wang,[2] Zhenfeng Lai,[2] Tao Kong,[2] Xia Wang,[2] Hongwen Ma,[1] Mingshu Yang[3]

[1]School of Materials Science and Technology, China University of Geosciences, Beijing, 100083, People's Republic of China
[2]Beijing Engineering Research Center of Architectural Functional Macromolecular Materials, Beijing Building Construction Research Institute, Co., Ltd., Beijing, 100039, People's Republic of China
[3]Beijing National Laboratory for Molecular Science, CAS Key Laboratory of Engineering Plastics, Institute of Chemistry, Chinese Academy of Sciences, Beijing 100190, People's Republic of China
Correspondence to: Q. X. Dong (E-mail: quanxiao185@iccas.ac.cn)

ABSTRACT: For the first time, expandable graphite (EG) and aluminum hydroxide (ATH) was combined to improve the flame retardancy of polyisocyanurate–polyurethane (PIR–PUR) foam. The limited oxygen index increased from 26.5 for the PIR–PUR matrix to an incredible value of 92.8 when 24 phr (parts per 100 of matrix) EG and 60 phr ATH were incorporated into the matrix. Based on morphology observation and thermogravimetric analysis, it was speculated that two factors contributed to the improvement of flame retardancy primarily. First, ATH could effectively induce "villi" like particles, which was useful to form a dense char. The compact char layer could effectively impede the transport of bubbles and heat. Second, ATH and EG accelerated the initial degradation and fluffy char was quickly generated on the surface of the composites. Thus, the degradation of the composite was slowed down and the diffusion of volatile combustible fragments to flame zone was delayed. © 2013 Wiley Periodicals, Inc. J. Appl. Polym. Sci. **2014**, *131*, 39936.

KEYWORDS: flame retardance; polyurethanes; thermal properties; foams; degradation

Received 10 May 2013; accepted 22 August 2013
DOI: 10.1002/app.39936

INTRODUCTION

Nowadays, polyurethanes have found wide applications in paints, adhesives, elastomers, flexible, and rigid foams, etc, and thus play an important and increasing role in industry and daily life.[1–3] In the last 30 years, concerns about energy conservation have led to a worldwide use of thermal insulators. In particular, rigid polyisocyanurate–polyurethane foams (PIR–PUR) have been widely used for insulation in construction and industrial applications due to their superior mechanical properties and low thermal conductivity. At the same time, the increasing public awareness of fire safety of materials, especially those used in construction and industrial applications, has also led to the approval of new regulations[4–6] and wide applications of flame retarded materials. Generally, the flame retardant property of materials could be improved by the incorporation of flame retardants. The common flame retardants used in PIR–PUR until now are phospho-halogenated compounds. However, those retardants generally cause very dense and toxic smokes during burning.[7,8] According to the new regulations of fire safety of materials, the density and toxicity of smoke are considered to be important factors for evaluating the fire safety of materials. For these reasons, there is an urgent demand to develop effective halogen-free flame retardants for polyurethane foams.[9–11]

Intumescent flame retardants (IFRs) are well known as a new generation of flame retardants because of their low smoke emission and toxic gases produced during burning and anti-dripping properties.[10] Conventional IFR systems are usually composed of three active ingredients, including acid source, blowing agent, and carbon source. Upon heating, these three active ingredients form a multicellular swollen char layer, which slows down the heat and mass transfer to interrupt the degradation of polymer matrix.[12–15] Several new IFR systems, such as the pentaerythritol based phosphate system,[16] the triazine-range based macromolecular charing agent system[17] and expandable graphite (EG),[18,19] have been investigated.

EG is an intercalated graphite compound in which some oxidants like sulfuric acid and potassium permanganate are included between the carbon layers of graphite.[20,21] When exposed to heat, EG expands and generates voluminous insulating layers, thus improving the flame retardancy of the polymeric

matrix. It has been reported that the expansion of EG occurs via a redox reaction between sulfuric acid and graphite[20]:

$$C + 2H_2SO_4 \rightarrow CO_2 + 2H_2O + 2SO_2$$

The blowing effect causes an increase of the volume of the materials by about 20,000–25,000% on heating to above 200°C. The "worm" like structure developed by graphite expansion suffocates the flame and the intumescent char layer formed limits the mass transfer from polymer to the heat source, preventing further decomposition of the material. However, low efficiency, high loading, and high cost are urgent issues, so it is imperative to develop novel and effective EG systems to reduce fire hazards and meet environmental protection standard for polyurethane foams.[19]

Over the last 10 years, researchers have paid great attention to the synergistic effect of organic and inorganic compounds, such as ammonium polyphosphate (APP),[22,23] triethylphosphate (TEP),[19] red phosphorus (RP),[24] and hydroxide flame retardant,[25,26] in EG systems to enhance the flame retardant efficiency. It was reported that EG and APP could improve the flame retardancy of rigid polyurethane foams.[23] With the incorporation of flame retardant of 15 wt %, the limited oxygen index (LOI) reached 30.5 at a weight ratio of 1 : 1 for EG and APP. It was attributed to the fact that the phosphoric acid generated from APP has good synergistic effect with EG in improving the char morphology. The char layer hindered the transfer of heat flow and combustible gases in the condensed phase. Modesti and Lorenzetti[24] studied PIR–PUR/EG/TEP composites with a density of about 0.038 g/cm^3 and found that PIR–PUR/EG (15 wt %) composites showed a LOI value of 25. By incorporating 3 wt % TEP into PIR–PUR/EG (15 wt %) matrix, the LOI value of the composite increased to 34. It was found that TEP and EG in the solid phase could induce a compact char layer, which prevented further decomposition of the underlying material. The effect of RP on the flame retardancy of PIR–PUR/EG systems was also studied by Modesti and Lorenzetti. [27] The fire behavior characterizations demonstrated that the incorporation of RP lead to a substantial improvement of the flame retardancy.

Hydroxide flame retardant,[25,26,28] such as aluminum hydroxide (ATH), magnesium hydroxide (MH), and layered double hydroxides (LDHs), are cheap, non-toxic, and smoke suppressing halogen-free flame retardant additives. The hydroxide flame retardants could also be used as a synergistic agent with EG to enhance the flame resistance of poly(ethylene–vinyl-acetate), polypropylene, etc.[25,26,28] However, to the best of our knowledge, there is no public report on the combining effect of hydroxide flame retardant and EG to improve the flame retardancy of PIR–PUR foams. In this study, the synergistic flame retardant effect of ATH for the EG flame-retarded PIR–PUR composites was studied and reported.

EXPERIMENTAL

Raw Materials and Sample Preparation

(1) A polyether polyol, 380A, made from poly(propylene oxide) and a sucrose/glycerin base, were purchased from Qingdao Lianmei Chemical Co. (Shandong, China). According to the manufacturer, the density of 380A is 1.15 g cm^{-3}, the typical hydroxyl number is 380 mg KOH equiv gram of resin, the functionality is 5.8 and the number average molecular weight is 700 g mol^{-1}. (2) Silicone glycol copolymer, used as a surfactant, was purchased from Shanghai Chemical Reagent Co. (Shanghai, China). (3) *N,N*-Dimethylcyclohexylamine, a catalyst with a density of 1.052 g cm^{-3}, was purchased from Sichuan Chemical Reagent Co. (Chengdu, China). (4) 1,1-Dichloro-1-fluoroethane (141 b), the blowing agent, and (5) dimethyl methylphosphonate, the flame retardant, were purchased from Qingdao Lianmei Chemical Co. (Shandong, China). (6) Polyisocyanate (PAPI) was obtained from Yantai Wanhua Polyurethanes Co. Manufacturer specifications shows that the polyisocyanate equivalent weight is 350 g, the –NCO content by weight is 30% and the functionality is 2.8. (7) Expandable graphites, with the particle size of about 50 μm, were kindly provided by Qingdao Baixing Graphite Co. (Shandong, China). (8) Aluminum hydroxide particles, with a particle size of 1–20 μm, were purchased from Beijing Chemical Factory and used without further purification.

Table I. Chemical Compositions of the PIR–PUR Matrix

Materials	Weight (g)
Polyether polyol (g)	100
Silicone glycol (g)	2
N,N-Dimethylcyclohexylamine (g)	2
1,1-Dichloro-1-fluoroethane (g)	15
Dimethyl methylphosphonate (g)	10
Polyisocyanate (g)	216

Unfilled PIR–PURs were prepared by conventional one-pot and free-rise method. Components (1)–(5) were mixed and mixed together and stirred using an electric stirrer until a uniform mixture was obtained at room temperature. The polyisocyanate (6) was then incorporated in, and the mixture was stirred for an additional 15 s. Chemical compositions of the PIR–PUR matrix are shown in Table I. Then the mixtures were poured into an aluminum cube with a dimension of 250 × 250 × 250 mm^3 and containing a paper cup. After that, the foams were placed in an oven at 70°C for 24 h, in order to complete the polymerization reaction. EG and ATH filled PIR–PUR composites were prepared similarly. EG particles were incorporated into the mixture just after components (1)–(5) were mixed. After the EG particles were completely wetted and dispersed in the mixture, ATH and polyisocyanate mixture were then incorporated in. The foam density was normalized to about 0.30 g/cm^3 by varying the dosage of 141b. The composites were prepared with a constant NCO index (300) in order to achieve greater thermal stability and better flame retardant behavior than polyurethane foams.

Characterizations

LOI was used to evaluate the flame retardancy of the PIR–PUR/EG/ATH composites. Specimens with dimension of 130 × 10 × 10 mm^3 were used to characterize LOI value using an oxygen

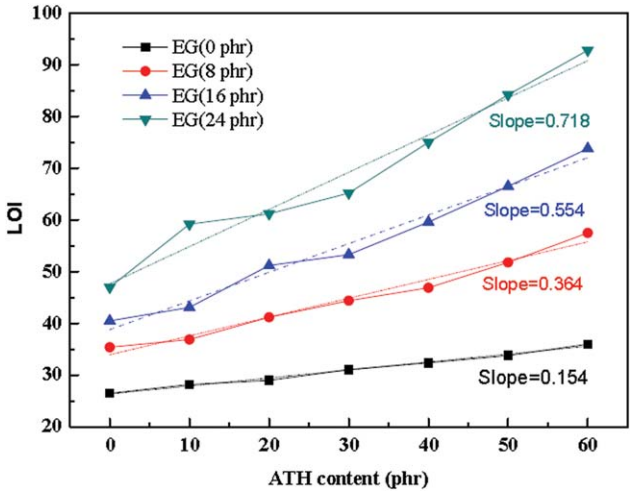

Figure 1. LOI curves of PIR–PUR/EG/ATH composites. [Color figure can be viewed in the online issue, which is available at wileyonlinelibrary.com.]

index meter (JF-3 Jiangning Analysis Instrument Factory, China) in accordance with ASTM D-2863. A JSM-6700F field emission Scanning Electron Microscope (SEM) was used to investigate the surface morphology of the char. About 3 mg of sample, taken from the internal region of the specimen, was used for thermogravimetric analysis (TGA) with a Perkin-Elmer TGA-7 under air atmosphere with an airflow of 25 mL/min from 50 to 750°C at a heating rate of 20°C/min.

RESULTS AND DISCUSSION

Flame Retardancy

Figure 1 gives the LOI curves of PIR–PUR/EG/ATH composites. When only EG or ATH was used, the LOI value did not change significantly. For example, the LOI value increased to 36 with a loading of 60 phr ATH into the PIR–PUR matrix. With the addition of 24 phr EG into the matrix, the LOI increased to 46 for PIR–PUR/EG composites (24 phr). However, the LOI value sharply increased to 92.8 when 24 phr EG and 60 phr ATH were incorporated into the PIR–PUR matrix (the total weight percent was 45.7%). This surprising result was due to the synergistic flame retarding effect of EG and ATH.

In Figure 1, keeping the EG content at a constant of 0, 8, 16, or 24 phr, different loadings of ATH were incorporated into the EG flame retarded PIR–PUR composites. Without EG, the LOI values of the PIR–PUR/ATH composites improved slightly as the loading of ATH increased, and the loading of 50 phr ATH was necessary to achieve LOI value of 33.8. The increment was only 7.3. It was interesting to note that slope of the LOI line increased to 0.718 with the incorporation of 24 phr EG into the matrix from 0.154 without incorporating EG. For example, the LOI value was 35.4 for PIR–PUR/EG_8/ATH_0 composites (the subscript number means the loading of flame retardant in the PIR–PUR matrix). While it increased to 51.8, with an improvement of 16.4, when 50 phr ATH were incorporated into PIR–PUR/EG_8 composites. Interestingly, the LOI value for the optimized flame retardant PIR–PUR/EG_{24}/ATH_{50} composites was 84.2, which was 38.2 higher than the PIR–PUR/EG_{24}/ATH_0 composites (LOI = 46). It was demonstrated that ATH had a good flame retarding effect in the PIR–PUR/EG systems. In comparison to the report in literatures, the highest LOI of PIR–PUR composites was less than 50,[19,29,30] which indicated that the reported 92.8 LOI value was the highest with only 45.7 wt % flame retardants (EG combined with ATH) into the matrix till now.

Thermal Properties

TGA was used to characterize thermal degradation in terms of mass loss. In Figure 2, it was found that thermal stability of the composites was enhanced with the incorporation of EG. Almost no residue was left for pure PIR–PUR foam at 750°C. The amount of residue improved to 23.6 wt % when 50 phr ATH and 4 phr EG were incorporated and increased to 32.4 wt % when 50 ATH phr and 24 phr EG were incorporated. For the DTG curves, it was found that T_{max1} (the temperature for maximum weight loss, i.e., the temperature at the first peak of the derivative TGA curve) decreased 20°C and the first weight loss rate increased as compared to that of the PIR–PUR matrix. However, the second weight loss rate decreased with increasing

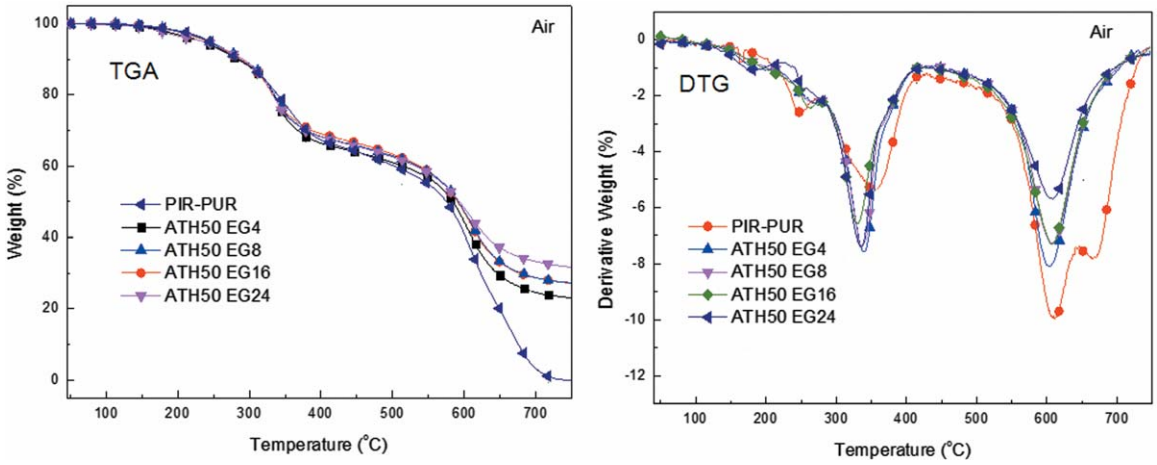

Figure 2. TGA (left) and DTG (right) curves of PIR–PUR/EG/ATH composites. [Color figure can be viewed in the online issue, which is available at wileyonlinelibrary.com.]

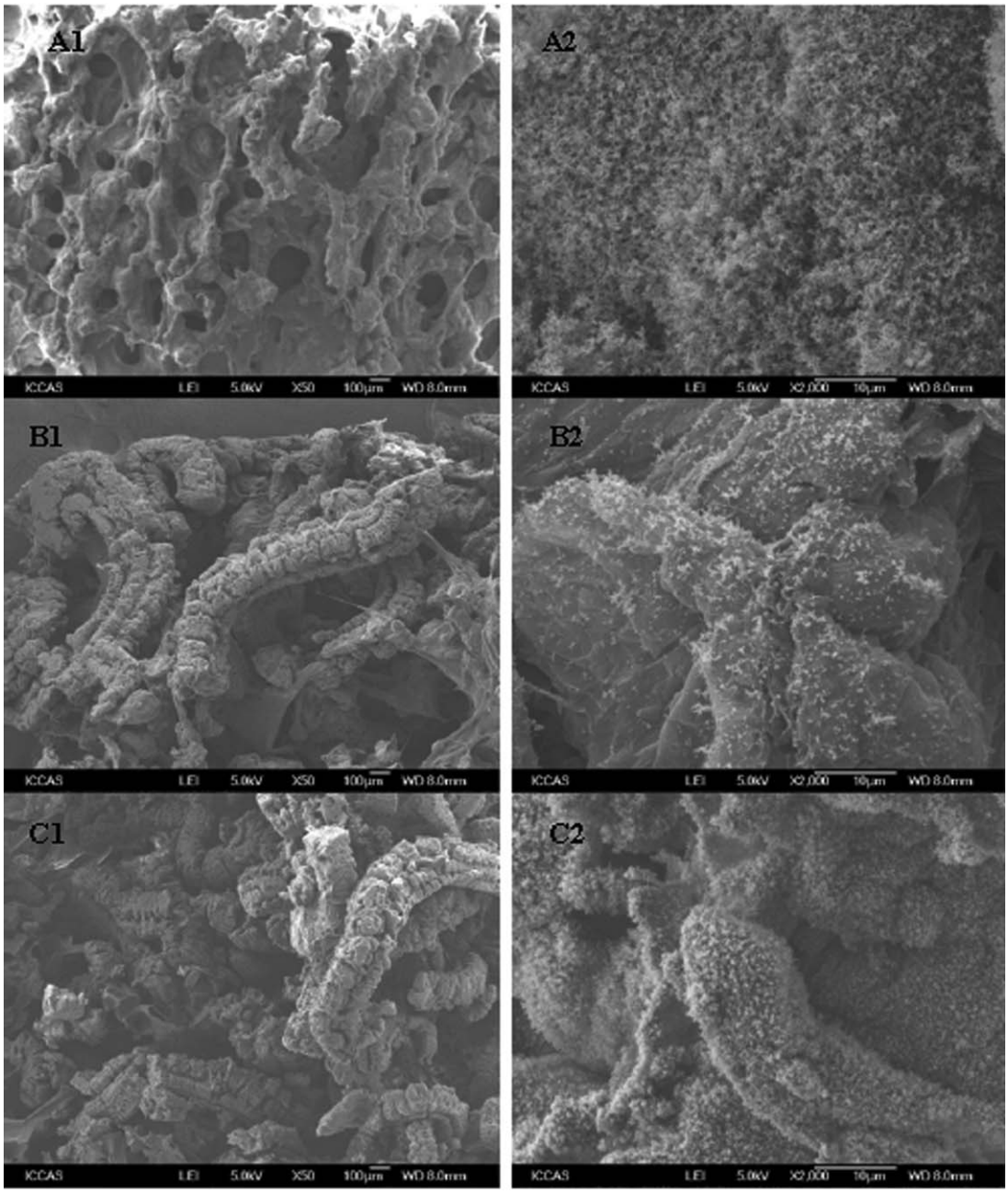

Figure 3. SEM images of the char layers: A1 and A2: PIR–PUR/ATH$_{60}$; B1 and B2: PIR–PUR/EG$_{24}$; C1 and C2: PIR–PUR/EG$_{24}$/ATH$_{60}$.

loading of EG. The reason was EG and ATH had low thermal stability, thus T_{max1} decreased and weight loss rate increased. After initial degradation, intumescent char generated, and the volatile combustible fragments by thermal degradation could slowly diffused and the weight loss rate decreased. With increasing of EG content, denser chars were generated and the weight loss rate decreased further.

Morphology of the Char

The morphology of char influences the flame retardancy and thermal stability of materials during burning. By SEM observation on the residue chars after LOI tests, it was possible to understand better how ATH and EG improved the flame retardancy of the matrix owing to the special char morphology. Figure 3 presents SEM images of the charred layers for PIR–PUR/ATH$_{60}$, PIR–PUR/EG$_{24}$ and PIR–PUR/EG$_{24}$/ATH$_{60}$ composites. In Figure 3(A1), the charred layers of the PIR–PUR/ATH$_{60}$ sample were thin and were constituted of numerous open holes [Figure 3(A2)]. Thus, heat transferred easily inside the sample and the flammable volatiles could penetrate the char layer into flame zone during combustion, resulting in moderate improved flame retardancy of the sample. However, tone can easily note an intumescent char layer with a "worms" like structure, deriving from the expansion of EG, as shown in Figures 3(B) and (C).

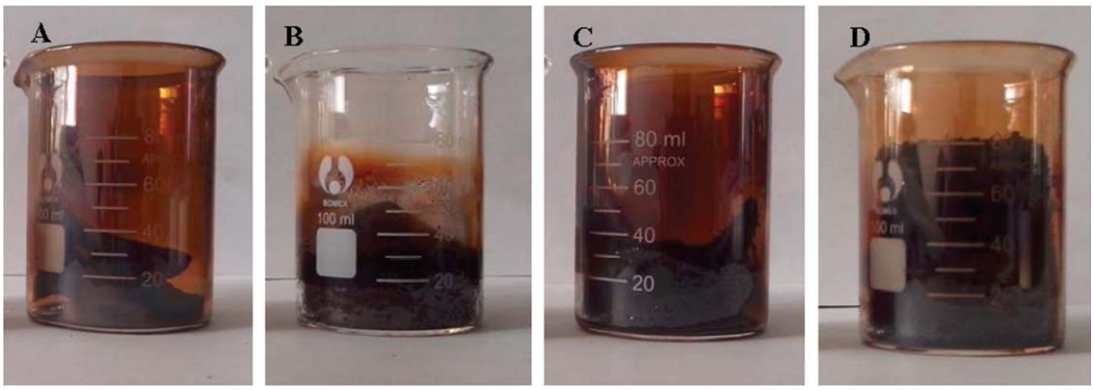

Figure 4. Morphological characteristics of the samples heated in a muffle furnace at 400°C for 10 min. (A) PIR–PUR; (B) PIR–PUR/ATH_{60}; (C) PIR–PUR/EG_{24}; (D) PIR–PUR/ATH_{60}/EG_{24}. [Color figure can be viewed in the online issue, which is available at wileyonlinelibrary.com.]

According to Modesti et al.,[19] the expansion of EG was due to a redox process between H_2SO_4 and the graphite that released the blowing gases. The blowing effect caused an increase of the volume of the materials by about 20,000–25,000% on heating above 200°C. The "worm" like structure developed by graphite expansion suffocated the flame and the intumescent char layer formed limited the heat and mass transfer from the polymer matrix to the heat source, preventing further decomposition of the materials. According to Huang et al, there are many small holes on the surface of expanded graphite. The size of these holes is about 50 nm to 1 μm.[24] At high magnification [Figure 3(B2)], it was found that the surface of expanded graphite was almost smooth. For the char of PIR–PUR/EG_{24}/ATH_{60} composites, "worm" like structures were also observed at low magnification [Figure 3(C1)]. It was surprising to note that many "villi" like particles were generated on the surface of expanded graphite [Figure 3(C2)]. The particles size was about 100 nm. It was speculated that the "villi" like particles could suffocate the small holes on the surface of expanded graphite, thus leading to more compact and dense char layers. This kind intumescent char layer could act as a heat insulation barrier and effectively impede the mass transfer of the degraded products between the polymer matrix and burning zone out of the surface. Thus, the generation of volatile combustible fragments by thermal degradation could be slowed down and less combustible products could diffuse to the flame zone, resulting in the improved LOI value to 92.8 when 24 phr EG and 60 phr ATH were simultaneously incorporated into the PIR–PUR matrix.

To simulate the thermal shock in the combustion, samples were packed as cylinder with a volume of 50 mL and then put into beakers and heated in a muffle furnace at 400°C for 10 min. In Figure 4(A), the residue was about 30 mL for the PIR–PUR sample and the beaker looked yellow, indicating the generation of much smoke during heating. The volume was to about 30 mL for PIR–PUR/ATH_{60} sample [Figure 4(B)]. It was interesting to note that top of the beaker was almost transparent, suggesting that ATH inhibited the smoke generation. It was reported water evaporation results in dilution of burning gases and Al_2O_3 formed on the burning polymeric surface protects the deeper layers of the polymer. It was assumed that Al_2O_3 enables absorption of the evolved smoke followed by chemical reaction with the metal oxides.[31,32] The phenomenon for the PIR–PUR/EG_{24} composites [Figure 4(C)] was similar as the PIR–PUR matrix [Figure 4(A)]. Surprisingly, a sensible swelling of the burned residue was visually observed and the volume increased to almost 80 mL for PIR–PUR/EG_{24}/ATH_{60} composites [Figure 4(D)]. It meant ATH and EG could synergistically induce intumescent char, which impeded the diffusion of volatile combustible fragments. Thus, more intumescent char layer was generated. This kind of intumescent charred layer could effectively prevent the mass transfer of degraded products between the polymer matrix and burning zone and thus improved flame-retardant property of the materials.

The mechanical properties of the PUR–PIR with different amount of ATH and EG are shown in Figure 5. The PUR–PIR composites with 8 phr EG and 20 phr ATH in the matrix had the highest strength. The compress strength increased to 0.65 MPa with incorporation of 20 phr ATH into PUR–PIR/EG (8 phr) composite (0.45 MPa), then decreased to 0.53 MPa with the addition of 50 phr ATH into the matrix. Similar trend was

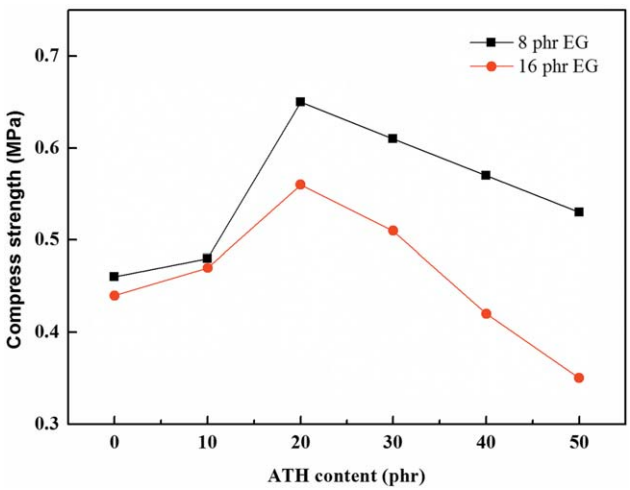

Figure 5. PIR–PUR composite with different EG and ATH loading. [Color figure can be viewed in the online issue, which is available at wileyonlinelibrary.com.]

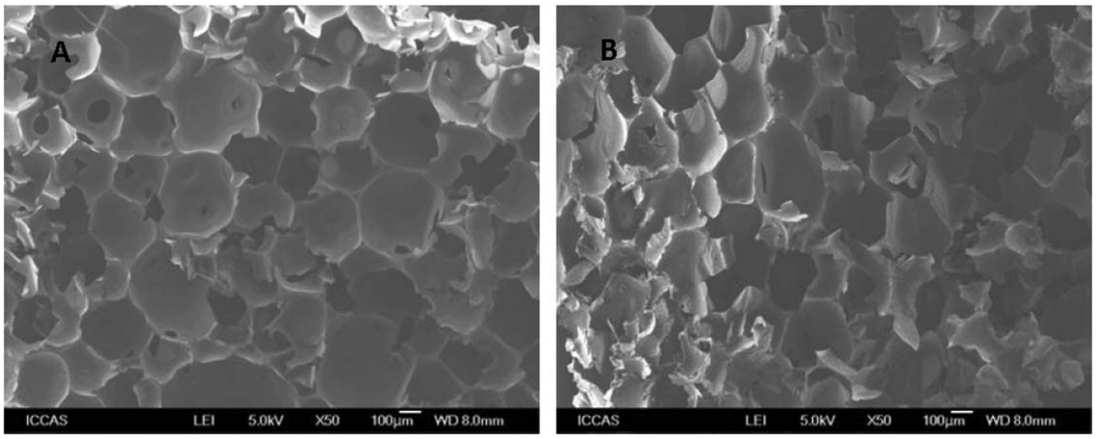

Figure 6. SEM of PIR–PUR foams with different ATH in the PIR–PUR/EG composites. (A) PIR–PUR /EG_{16}/ATH_{20}; (B) PIR–PUR/EG_{16}/ATH_{50}.

observed for PUR–PIR composite with incorporation of 16 phr EG in the matrix. SEM was used to investigate the foam morphology (Figure 6). It was found that pore size was almost uniform with incorporation of 20 phr ATH in the matrix (Figure 6A). However, the pore structure was broken when ATH loading increased to 50 phr (Figure 6B). It was speculated that ATH might act as nucleating agent during the formation of PIR–PUR foams. When the loading was low, ATH could well distribute in the matrix, thus the pore size was almost uniform. But agglomerates generated when ATH loading was high. The pore structure was destroyed and mechanical strength decreased with increasing incorporation of ATH into the matrix.

CONCLUSION

The synergistic effect of EG combined with ATH on flame retardancy of PIR–PUR was firstly investigated. The LOI value of PIR–PUR/EG_{24}/ATH_{60} composites increased to 92.8 with incorporation of both 60 phr ATH and 24 phr EG into the matrix. TGA results indicated that ATH and EG could synergistically induce the initial degradation and quickly form intumescent char, thus volatile combustible fragments by thermal degradation could be slowed down and less combustible products diffused to the flame zone. SEM characterization suggested that ATH could effectively induce "villi" like particles generation on the surface of expandable graphite. The "villi" like particles could make the char layers more compact and dense. This kind intumescent char layer could act as a heat insulation barrier and effectively impede the mass transfer of degraded products between the polymer matrix and burning zone out of the surface. Thus, the generation of volatile combustible fragments by thermal degradation could be slowed down and less combustible products diffused to the flame zone, which was benefited to increase the flame retardancy.

ACKNOWLEDGMENTS

This study was financially supported by opening funding of Beijing National Laboratory for Molecular Sciences (BNLMS) and the Youth Foundation of Beijing Building Construction Research Institute, Co., Ltd. Dr. Quanxiao Dong thanks the financial support of postdoctoral program in Beijing Construction Engineering Group Co., Ltd. Wanjin Wang and Kui He found the flame retardancy property and wrote most of the manuscript. Dr. Quanxiao Dong supervised this research and revised the manuscript. Ning Zhu, Yong Fan, Feng Wang, and Yibing Xia performed the TGA experiments, muffle furnace, and LOI tests. Haifeng Li, Jing Wang, and Zhen Yuan did the mechanical and SEM characterizations. Erpo Wang, Zhenfeng Lai, Tao Kong, and Xia Wang made contribution to investigating different formulations, such as polyol, catalyst, polyisocyanate etc, of the PIR–PUR basic matrix. Prof. Hongwen Ma and Mingshu Yang provided useful information for the mechanism explanation.

REFERENCES

1. Chattopadhyay, D. K.; Raju, K. *Prog. Polym. Sci.* **2007**, *32*, 352.
2. Ravey, M.; Weil, E. D.; Keidar, I.; Pearce, E. M.; *J. Appl. Polym. Sci.* **1998**, *68*, 231.
3. Liaw, D. J. *J. Appl. Polym. Sci.* **1997**, *66*, 1251.
4. Chattopadhyay, D. K.; Webster, D. C. *Prog. Polym. Sci.* **2009**, *34*, 1068.
5. Modesti, M.; Lorenzetti, A.; Simioni, F.; Checchin, M. *Polym. Degrad. Stab.* **2001**, *74*, 475.
6. Lorenzetti, A.; Modesti, M.; Gallo, E.; Schartel, B.; Besco, S.; Roso, M. *Polym. Degrad. Stab.* **2012**, *97*, 2364.
7. Levchik, S. V.; Weil, E. D. *J. Fire Sci.* **2006**, *24*, 345.
8. Singh, H.; Jain, A. K.; *J. Appl. Polym. Sci.* **2009**, *111*, 1115.
9. Modesti, M.; Lorenzetti, A. *Eur. Polym. J.* **2003**, *39*, 263.
10. Zhang, P.; Song, L.; Lu, H. D.; Wang, J. A.; Hu, Y. A. *Ind. Eng. Chem. Res.* **2010**, *49*, 6003.
11. Yuan, C. Y.; Chen, S. Y.; Tsai, C. H.; Chiu, Y. S.; Chen-Yang, Y. W. *Polym. Adv. Technol.* **2005**, *16*, 393.
12. Cao, K.; Wu, S. L.; Wang, K. L.; Yao, Z. *Ind. Eng. Chem. Res.* **2011**, *50*, 8402.
13. Chen, M. J.; Shao, Z. B.; Wang, X. L.; Chen, L.; Wang, Y. Z. *Ind. Eng. Chem. Res.* **2012**, *51*, 9769.

14. Song, P. A.; Xu, L. H.; Guo, Z. H.; Zhang, Y.; Fang, Z. P. *J. Mater. Chem.* **2008**, *18*, 5083.
15. Lu, H. D.; Wilkie, C. A. *Polym. Adv. Technol.* **2011**, *22*, 1123.
16. Song, P. A.; Fang, Z. P.; Tong, L. F.; Xu, Z. B. *Polym. Eng. Sci.* **2009**, *49*, 1326.
17. Wang, X.; Hu, Y.; Song, L.; Xing, W. Y.; Lu, H. D.; Lv, P.; Jie, G. X. *Polym. Adv. Technol.* **2011**, *22*, 2480.
18. Duquesne, S.; Le Bras, M.; Bourbigot, S.; Delobel, R.; Poutch, F.; Camino, G.; Eling, B.; Lindsay, C.; Roels, T. *J. Fire Sci.* **2000**, *18*, 456.
19. Modesti, M.; Lorenzetti, A.; Simioni, F.; Camino, G. *Polym. Degrad. Stab.* **2002**, *77*, 195.
20. Ge, L. L.; Duan, H. J.; Zhang, X. G.; Chen, C.; Tang, J. H.; Li, Z. M. *J. Appl. Polym. Sci.* **2012**, *126*, 1337.
21. Wang, H. F.; Li, B. *Polym. Adv. Technol.* **2010**, *21*, 691.
22. Wang, B. B.; Hu, S.; Zhao, K. M.; Lu, H. D.; Song, L.; Hu, Y. *Ind. Eng. Chem. Res.* **2011**, *50*, 11476.
23. Meng, X. Y.; Ye, L.; Zhang, X. G.; Tang, P. M.; Tang, J. H.; Ji, X.; Li, Z. M. *J. Appl. Polym. Sci.* **2009**, *114*, 853.
24. Modesti, M.; Lorenzetti, A. *Polym. Degrad. Stab.* **2002**, *78*, 341.
25. Chen, X. L.; Wu, H.; Luo, Z.; Yang, B.; Guo, S. Y.; Yu, J. *Polym. Eng. Sci.* **2007**, *47*, 1756.
26. Li, Z. Z.; Qu, B. J. *Polym. Degrad. Stab.* **2003**, *81*, 401.
27. Modesti, M.; Lorenzetti, A. *Polym. Degrad. Stab.* **2002**, *78*, 167.
28. Jiao, C. M.; Wang, Z. Z.; Ye, Z.; Hu, Y.; Fan, W. C. *J. Fire Sci.* **2006**, *24*, 47.
29. Shi, L.; Li, Z. M.; Xie, B. H.; Wang, J. H.; Tian, C. R.; Yang, M. B. *Polym. Int.* **2006**, *55*, 862.
30. Shi, L.; Li, Z. M.; Yang, M. B.; Yin, B.; Zhou, Q. M.; Tian, C. R.; Wang, J. H. *Polym. Plast. Technol. Eng.* **2005**, *44*, 1323.
31. Levchik, S. V.; Weil, E. D. *Polym. Adv. Technol.* **2005**, *16*, 707.
32. Yeh, J. T.; Hsieh, S. H.; Cheng, Y. C.; Yang, M. J.; Chen, K. N. *Polym. Degrad. Stab.* **1998**, *61*, 399.